Andreev bound state and multiple energy gaps in the noncentrosymmetric superconductor BiPd

Mintu Mondal,[1] Bhanu Joshi,[1] Sanjeev Kumar,[1] Anand Kamlapure,[1] Somesh Chandra Ganguli,[1] Arumugam Thamizhavel,[1] Sudhansu S. Mandal,[2] Srinivasan Ramakrishnan,[1,*] and Pratap Raychaudhuri[1,†]

[1]*Tata Institute of Fundamental Research, Homi Bhabha Road, Colaba, Mumbai 400005, India*

[2]*Department of Theoretical Physics, Indian Association for the Cultivation of Science, Jadavpur, Kolkata-700032, India*

(Received 27 February 2012; revised manuscript received 28 May 2012; published 18 September 2012)

We report directional point contact Andreev reflection (PCAR) measurements on high-quality single crystals of the noncentrosymmetric superconductor BiPd. The PCAR spectra measured on different crystallographic faces of the single crystal clearly show the presence of multiple superconducting energy gaps. For point contacts with low resistance, in addition to the superconducting gap feature, a pronounced zero-bias conductance peak is observed. These observations provide strong evidence for the presence of an unconventional order parameter in this material.

DOI: 10.1103/PhysRevB.86.094520 PACS number(s): 74.20.Rp, 74.45.+c, 74.70.Ad, 74.20.Mn

The discovery of superconductivity in the noncentrosymmetric superconductor[1] (NCS) $CePt_3Si$ has generated widespread interest in this class of systems. In superconductors where inversion symmetry is present, the superconducting order parameter (OP) is characterized by a distinct parity corresponding to either a spin-singlet or a spin-triplet pairing. However in NCSs, the lack of inversion symmetry combined with antisymmetric (Rashba-type) spin-orbit coupling (ASOC)[2] can cause an admixture of the spin-singlet and spin-triplet pairing.[3] In the simplest situation of a single band contributing to superconductivity, this mixing is expected to give rise to a two-component OP. In a real system, the order parameter would, therefore, have two or more components, depending on the complexity of the Fermi surface, giving rise to unusual temperatures and field dependences of superconducting parameters.[4–11]

Despite numerous theoretical predictions, experimental evidence of an unconventional superconducting state in NCSs has been very few, possibly due to the small spin-orbit coupling. Thus, the vast majority of NCSs, (e.g., Re_3W, $Mg_{10}Ir_{19}B_{16}$, Mo_3Al_2C, and $Re_{24}Nb_5$) display predominantly conventional s-wave behavior and occasionally multiband superconductivity.[12–15] In some systems, such as $CePt_3Si$ (Ref. 16) and UIr (Ref. 17), the study of parity-broken superconductivity is complicated by strong electronic correlations and by the coexistence of magnetism. One notable exception is Li_2Pt_3B in which penetration depth[18,19] and nuclear-magnetic-resonance[20] measurements provide evidence for the existence of nodes in the gap function. However, a direct spectroscopic evidence for the presence of an unconventional order parameter has not been reported for any of these materials.

In this paper, we report directional point contact Andreev reflection (PCAR) measurements on a BiPd single crystal (Ref. 21), which is a recent addition to the family of NCSs. Since the spin-orbit coupling depends on the square of the atomic number (Z) of the elements involved, the presence of Bi ($Z = 83$) is expected to result in a large spin-orbit coupling in this material. BiPd has a monoclinic crystal structure with lattice constants $a = 5.63$, $b = 10.66$, $c = 5.68$ Å, $\alpha = \gamma = 90^\circ$, and $\beta = 101^\circ$. Recent thermodynamic and transport measurements[21] on high-quality BiPd single crystals (residual resistivity, $\rho \sim 0.3\ \mu\Omega$ cm and residual resistivity ratio $\sim$160) revealed that the specific heat jump at T_c is smaller than expected for a BCS superconductor, suggesting the possibility of multiple superconducting order parameters in this material.

Directional PCAR spectroscopy,[22] i.e., where the conductance spectra (dI/dV versus V) are recorded by injecting a current from a normal metal through a ballistic point contact along different crystallographic directions in the superconductor, is a powerful tool to investigate the gap anisotropy in superconductors.[23,24] In this paper, PCAR spectra were recorded on a BiPd single crystal by injecting a current (I) either along b ($I \parallel b$) or perpendicular to b ($I \perp b$). The central observation from these studies is the presence of a pronounced zero-bias conductance peak (ZBCP) in both crystallographic directions, which coexists with more conventional gaplike features. Our results strongly suggest that a spin-triplet OP coexists with a spin-singlet OP in this material.

A high-quality BiPd single crystal was grown by the modified Bridgman technique (for details about crystal growth, see Ref. 21). The directional point contact measurements were performed on a piece of single crystal cut into a rectangular parallelepiped shape of size 1 mm $\times$ 1.5 mm $\times$ 2 mm, which had large well-oriented faces on the (010) and (001) planes. The superconducting transition temperature $T_c \sim 3.62$ K of the crystal was determined by measuring ac susceptibility at 60 kHz using a two-coil mutual inductance technique.[25] From the resistivity and specific heat measurements on a similar crystal, we estimate the electronic mean-free path[21] $l \sim 2.4\ \mu$m at low temperatures. The quality of the crystal was also confirmed by observing de Haas–van Alphen oscillation.[26] Before performing the point contact measurement, the crystal surface was polished to a mirror finish. To make ballistic point contact, a mechanically cut fine tip made from 0.25-mm diameter Ag wire was brought in contact with the crystal using a differential screw arrangement in a conventional sample-in-liquid ^{3}He cryostat. Measurements were performed by making the contact on two different crystal faces: (i) (010) corresponding approximately to $I \parallel b$ and (ii) (001) corresponding approximately to $I \perp b$. I-V characteristics of the junction formed between the tip and the sample were measured at different temperatures down to $T = 0.4$ K using a conventional four-probe technique. The dI/dV versus V spectra were obtained by numerically differentiating the I-V

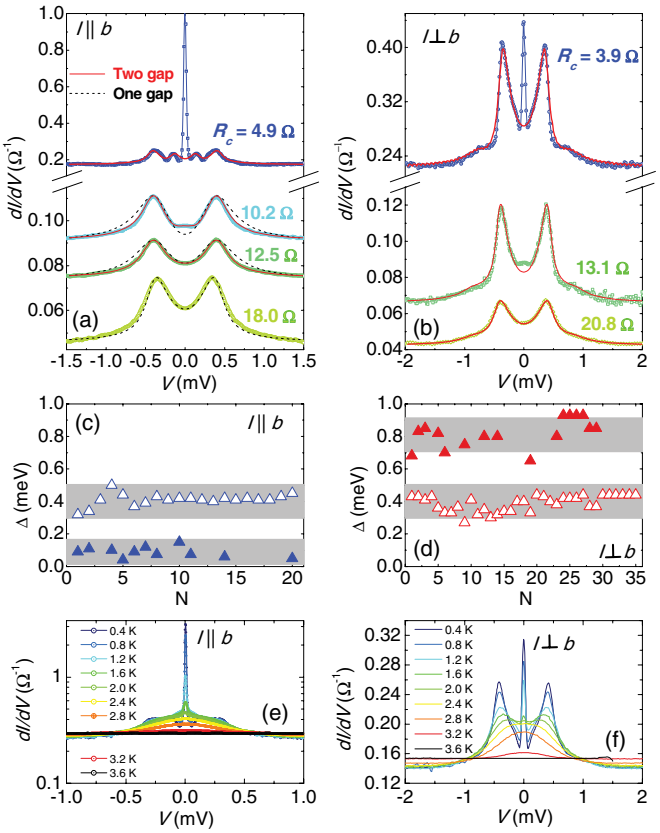

FIG. 1. (Color online) PCAR spectra for different contact resistances at $T \sim 0.35$ K: (a) $I \parallel b$ and (b) $I \perp b$. Solid lines (red) are fits to the modified two-gap BTK model. The corresponding fits with a single-gap model (black dashed lines) are also shown for comparison for some of the spectra. (c) and (d) Scatter plots of a superconducting energy gap obtained by fitting the modified BTK model to the experimental PCAR spectra for $I \parallel b$ and $I \perp b$ plotted as a function of the serial number of the spectra. The bands are guides to the eye. (e) and (f) Temperature dependence of the PCAR spectra for two low R_c contacts for $I \parallel b$ and $I \perp b$, respectively.

curves. For all spectra reported here, the contact resistance (R_c) in the normal state varied in the range of $R_c \sim 1$–$30\ \Omega$. The corresponding contact diameter estimated using the Sharvin formula,[27] $d = (\frac{4\rho l}{3\pi R_c})^{1/2} \sim 100$–$500$ Å was much smaller than l. Therefore, all our point contact spectra are taken in a ballistic limit. To further understand the nature of superconductivity, we have measured the upper critical field (H_{c2}) and its anisotropy along two crystallographic axes ($H \parallel b$ and $H \perp b$) by measuring ac susceptibility as a function of the magnetic field at different temperatures.

We first concentrate on the PCAR spectra at the lowest temperature. From a considerable amount of statistics, we observe two kinds of PCAR spectra, corresponding to $I \parallel b$ and $I \perp b$, respectively.[28] Figures 1(a) and 1(b) show representative evolution with R_c of the (dI/dV) versus V spectra for $I \parallel b$ and $I \perp b$, respectively. In both directions, the striking feature is the observation of a pronounced ZBCP, which coexists with more conventional gaplike features in the low R_c contacts. In addition, for $I \parallel b$, clear coherence peaks associated with superconducting gaps are observed around 0.1 and 0.4 meV, respectively. For $I \perp b$, the corresponding structures are observed at 0.4 and 0.8 meV, respectively. As the contact resistance is increased by gradually withdrawing the tip in both directions, the ZBCP slowly vanishes, and we recover spectra with only gaplike features. To quantitatively obtain the values of the superconducting energy gaps, we fit the spectra using a two-band Blonder-Thinkham-Klapwijk (BTK) model[29,30] generalized to take into account broadening effects. In this model, the normalized conductance $[G(V)/G_N$, where $G_N = G(V \gg \Delta)]$ is a weighted sum of the conductance of two transport channels $[G_1(V)$ and $G_2(V)]$ arising from the two order parameters: $G(V)/G_N = (1-w)G_1(V)/G_{1N} + wG_2(V)/G_{2N}$. $G_1(V)/G_{1N}$ and $G_2(V)/G_{2N}$ are calculated using the generalized BTK formalism using the relative weight factors of the two gaps (w), superconducting energy gaps (Δ_1 and Δ_2), the barrier potentials (Z_1 and Z_2), and the broadening parameters (Γ_1 and Γ_2) as fitting parameters. All spectra can be fitted very well with this two-band model if we neglect the large ZBCP that arises for contact with low R_c. Analyzing more than 50 spectra along $I \parallel b$ and $I \perp b$ [Figs. 1(c) and 1(d)], we observed that the dominant feature is a gap $\Delta_1 \sim 0.4 \pm 0.1$ meV, present along both directions. For $I \parallel b$, in about 50% of the spectra, we can clearly resolve a smaller gap $\Delta_2 \sim 0.1 \pm 0.05$ meV with $w \sim 0.2$–0.6. On the other hand, in 50% of the spectra along $I \perp b$, we can clearly resolve a larger gap $\Delta_3 \sim 0.8 \pm 0.15$ meV with $w \sim 0.1$–0.35. We did not obtain any spectra showing the three gaps simultaneously in the same spectra. The large variation in w and the dispersion in gap values arise from surface roughness, which limits our inability to precisely inject a current along a desired direction. Figures 1(e) and 1(f) show the temperature dependence of the PCAR spectra for two representative low-R_c contacts, corresponding to $I \parallel b$ and $I \perp b$, respectively. The ZBCP decreases with increasing temperature and disappears at about $0.7T_c$. At T_c (3.6 K), the spectra are featureless, and the conductance is independent of bias voltage.

To obtain the temperature variation in the superconducting energy gaps, we analyze the temperature dependence of two point contacts along the two directions with large R_c (Fig. 2) where the ZBCP is suppressed. Consistent with the notation used for the superconducting energy gaps, we denote the barrier parameters and the broadening parameters as Z_1 and Γ_1 (associated with Δ_1), Z_2 and Γ_2 (associated with Δ_2) and, Z_3, Γ_3 (associated with Δ_3). A comparison between the single- and the two-gap fits [Figs. 2(a) and 2(d)] of the spectra at the lowest temperatures shows that a single gap is clearly inadequate to fit the spectra. Figures 2(b) and 2(e) show the two-gap fits of the spectra at various temperatures for $I \parallel b$ and $I \perp b$, respectively. As expected, Z_1, Z_2, and Z_3 [Figs. 2(g) and 2(h)] are temperature independent[31] for both $I \parallel b$ and $I \perp b$. The temperature variation in Γ_1, Γ_2, and Γ_3, on the other hand, is more complicated. Formally, the broadening parameters are introduced as an inverse lifetime[32] of the excited quasiparticles. From this perspective, one expects this parameter to be small at low temperatures and to increase close to T_c due to recombination of electron and holelike Bogoliubons. This is consistent with the temperature variation in Γ_1 in both Figs. 2(g) and 2(h). However, Γ_2 and Γ_3 decrease with temperature. To understand this discrepancy, we note that, phenomenologically, the broadening parameters

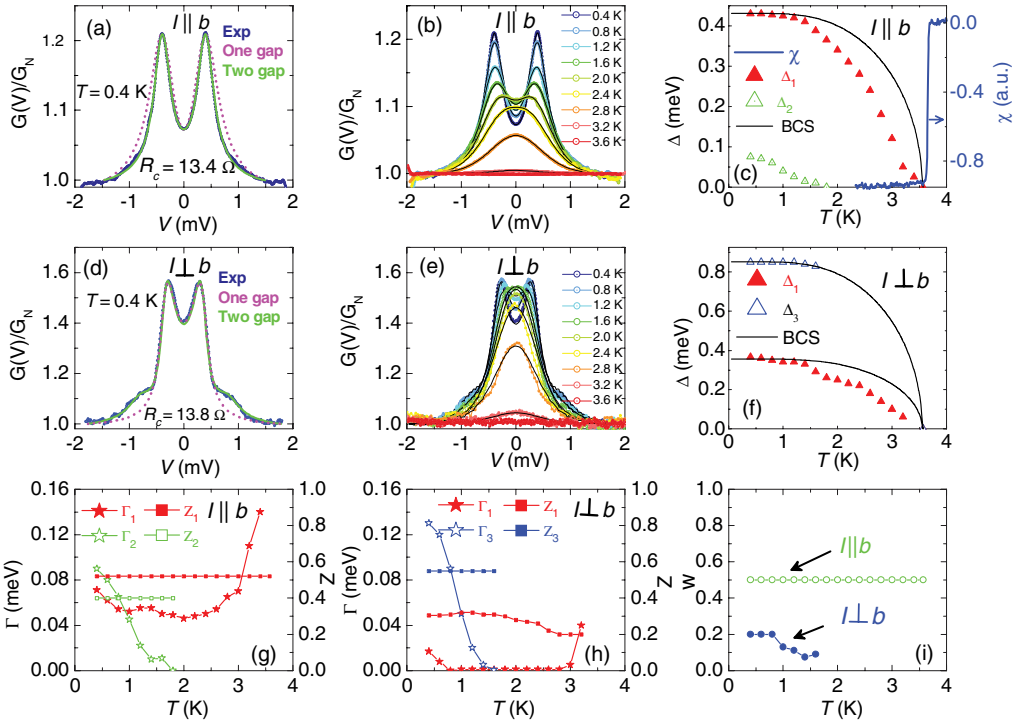

FIG. 2. (Color online) Comparison between one-gap and two-gap fits for PCAR spectra recorded at the lowest temperature for (a) $I \parallel b$ and (d) $I \perp b$. Temperature variation in the PCAR spectra for (b) $I \parallel b$ and (e) $I \perp b$. (c) and (f) show the temperature dependence of the superconducting energy gaps extracted from (b) and (e), respectively; the solid black lines are the expected BCS variation in Δ. (g) and (h) show the temperature variation in the broadening parameters and the barrier parameters obtained from the best fits of the spectra in (b) and (e), respectively. (i) Temperature variation in the relative weight factor (w) for the two gaps used in the best fit of the spectra in (b) and (e). The blue solid line in panel (c) shows the real part of the ac susceptibility (χ) as a function of temperature showing the superconducting transition of BiPd.

take into account all nonthermal sources of broadening, such as a distribution of gap function resulting from an anisotropic gap function[23] and instrumental broadening. For a strongly anisotropic gap function, with an increase in temperature, intraband scattering can partially smear out the gap anisotropy thereby causing the broadening parameter to decrease. In the present case, we can also not rule out the possibility that the discrepancy is an artifact arising from the fact that our fits assume k-independent Δ_1 and Δ_2 where the anisotropy of the gap functions is ignored. Figures 2(c) and 2(f) show the temperature dependence of Δ_1, Δ_2, and Δ_3, and Fig. 2(i) shows the relative weight factors corresponding to the two-gap fits. It is instructive to note that Δ_1 has a similar temperature variation for both $I \parallel b$ and $I \perp b$ and closes at T_c, confirming that this gap is associated with the same gap function. For $I \parallel b$, w remains constant with temperature, whereas, Δ_2 decreases rapidly at low temperatures and forms a tail towards T_c as expected for a multiband superconductor. For $I \perp b$, w decreases with increasing temperature, and above 1.6 K, all the spectra can be effectively fitted with a single gap Δ_1.

We now focus on the origin of the ZBCP in the low-resistance spectra. Since ZBCP can arise from several origins, it is important to analyze the observed ZBCP in BiPd critically. First, we look for extrinsic origins of the ZBCP that are not associated with genuine spectroscopic features. It has been shown that, in the case where the point contact is not purely in the ballistic limit, ZBCP can arise from the current reaching the critical current[33] (I_c) of the point contact. However, in our case, such a possibility can be trivially ruled out for two reasons. First, as we have shown before, our contact is well in the ballistic limit even after considering the error associated with our determination of contact diameter from R_c. More importantly, the conductance spectra at currents larger than I_c cannot contain any spectroscopic information. In our case, however, we observe clear signatures of the superconducting energy gap at bias voltages much higher than the voltage range where the ZBCP appears. Other origins of ZBCP include (i) magnetic scattering,[34,35] (ii) proximity-induced pair tunneling[36] (PIPT), and (iii) the Andreev bound state[7,37] (ABS) when the superconductor has an unconventional symmetry. The ZBCP resulting from magnetic scattering is expected to split under the application of magnetic field, and PIPTs should get suppressed at small fields on the order of 0.1 T. In Figs. 3(a) and 3(b), we show the evolution of the ZBCP with the magnetic field (H) applied perpendicular to the junction (i.e., $H \parallel I$) for two contacts with $I \parallel b$ and $I \perp b$, respectively. Unlike the case when H is parallel to the junction, for this orientation of H, the ZBCP arising from the ABS is not expected to split but gradually reduces and disappears at high fields. We observe that the ZBCP for both $I \parallel b$ and $I \perp b$ persists at moderately high fields and does not show any splitting with the magnetic field. This effectively rules out magnetic scattering and PIPT as origins of the ZBCP but is consistent with the expectation for ABSs. We would also like

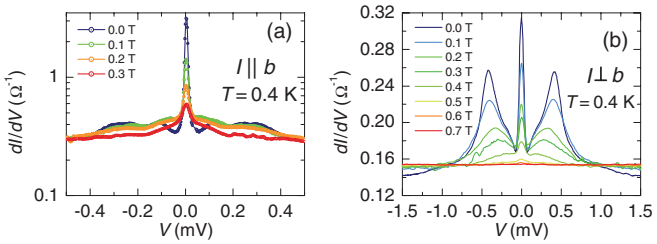

FIG. 3. (Color online) Magnetic-field dependence of PCAR spectra showing the ZBCP for two point contacts with (a) $I \parallel b$ and (b) $I \perp b$. The spectra are measured at 0.4 K.

to point out that, although the narrow ZBCP observed in our experiments has a superficial similarity with that originating from the Josephson effect in a superconductor-superconductor tunnel junction, such a possibility is extremely remote in our experimental configuration where the contact is established between a normal metal tip and a superconducting single crystal. Although it is possible for some contacts to form accidental grain boundary Josephson junctions through a tiny broken piece of the crystal, which comes in a series during the contact formation process, it is statistically impossible for this to happen for all large area contacts that we have measured in the course of this paper. We, therefore, conclude the ZBCPs observed here are manifestations of the ABS originating from an unconventional component of the order parameter in this material. Further confirmation of the ABS origin of the ZBCP comes from its evolution with contact size. Since the mean size of the ABS is on the order of the dirty limit coherence length (ξ_0), the ZBCP originating from the ABS gradually disappears as the contact diameter becomes smaller than ξ_0. From the upper critical field (H_{c2}) measured with $H \parallel b$ and $H \perp b$ [Fig. 4(b)], assuming the simplest situation of a triangular Abrikosov vortex lattice existing in BiPd, we estimate ξ_0 to be on the order of 20 and 17 nm, respectively. In Fig. 4(a), we plot the height of the ZBCP (defined as the difference between the experimental zero-bias conductance and the zero-bias conductance obtained from the generalized two-band BTK fit) as a function of d calculated

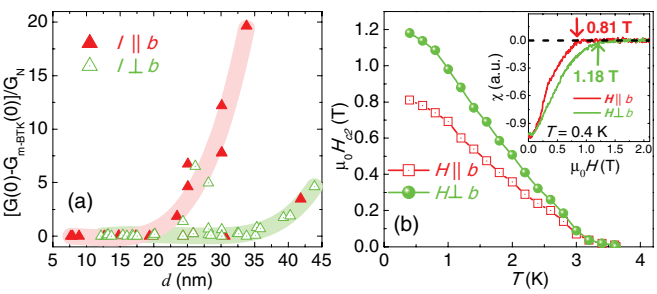

FIG. 4. (Color online) (a) Height of the ZBCP measured at 0.4 K as function of contact diameter d. The solid triangles (red) correspond to $I \parallel b$, and the open triangles correspond to $I \perp b$. The thick shaded lines are guides to the eye. It shows two branches of points associated with the ABS in two different directions. (b) H_{c2} as a function of temperature (T) for $H \parallel b$ and $H \perp b$. The inset shows ac susceptibility as a function of the magnetic field at $T = 0.4$ K. The H_{c2} (shown by arrows) has been extracted from susceptibility data taken as a function of the magnetic field at different temperatures.

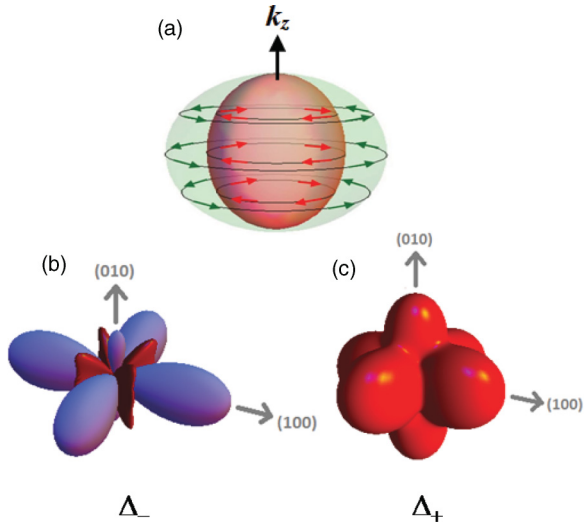

FIG. 5. (Color online) (a) Schematic of the spin-split Fermi surface due to spin-orbit coupling, forming the + (outer surface) and − (inner surface) helicity bands. The spin eigenstates (shown by arrows) point parallel and antiparallel to $\boldsymbol{g}(\boldsymbol{k})$, respectively. (b) and (c) One possible realization of the gap functions corresponding to Δ_- and Δ_+ corresponding to a particular choice of the vector $\boldsymbol{g}(\boldsymbol{k})$. Darker (red) and lighter (blue) regions correspond to positive and negative values of the gap function, respectively. Note that the small monoclinic distortion of BiPd has been neglected in the symmetry of the gap functions.

using the Sharvin formula.[27] The ZBCP disappears for $d \lesssim 20$ and $d \lesssim 32$ nm for $I \parallel b$ and $I \perp b$, respectively.[38] We believe that the slightly larger critical diameter for $I \perp b$ compared to ξ_0 results from several approximations used in this analysis. First, the determination of d from R_c is necessarily an approximation, which does not take into account the irregular shape of a real contact or the effect of the barrier potential that could exist between the tip and the superconductor. Second, the determination of ξ_0 assumes a triangular vortex lattice, which might not necessarily be the case for a superconductor with unconventional pairing symmetry. Considering the errors involved with these approximations and the fact that the criterion for the disappearance of the ZBCP with contact size is only valid within a factor on the order of unity, the qualitative trend of the ZBCP with d is in excellent agreement with the theoretical expectation for the ABS. We, therefore, conclude that the ZBCP in BiPd originates from the ABS resulting from an unconventional OP for which the phase varies on the Fermi surface.

We can now put these observations in the proper perspective. For a NCS, ASOC leads to a term of the form $\alpha \boldsymbol{g}(\boldsymbol{k}) \cdot \sigma$ in the Hamiltonian, where α is the spin-orbit coupling constant, σ is the Pauli matrices, and the vector $\boldsymbol{g}(\boldsymbol{k})$, representing the orbital direction, obeys the antisymmetric property such that $\boldsymbol{g}(\boldsymbol{k}) = -\boldsymbol{g}(-\boldsymbol{k})$. In general, the explicit form of $\boldsymbol{g}(\boldsymbol{k})$ is determined by details of the crystal structure. The ASOC breaks the spin degeneracy, which leads to two bands characterized by $\pm$ helicities for which the spin eigenstates are either parallel or antiparallel to $\boldsymbol{g}(\boldsymbol{k})$. This is schematically illustrated in Fig. 5. These helicity eigenstates are, therefore,

coherent superpositions of spin-up and spin-down eigenstates. The superconducting gap functions for the intraband pairs are $\Delta_+(\boldsymbol{k})$ and $\Delta_-(\boldsymbol{k})$ for the respective helicity bands [Figs. 5(b) and 5(c)]. When the ASOC is large, interband pairing is suppressed, and in such a case, the superconducting transition temperature is maximized[6] when the quantization direction of the triplet symmetry becomes parallel to $\boldsymbol{g}(\boldsymbol{k})$. Since the pairing occurs between intraband electrons only and the bands are of helicity eigenstates, the superconducting gap function is an admixture of spin-singlet and spin-triplet symmetries: $\Delta(\boldsymbol{k}) = [\Delta_s(\boldsymbol{k})\mathbf{I} + \Delta_t(\boldsymbol{k})\hat{g}(\boldsymbol{k}) \cdot \sigma](i\sigma_y)$, where $\mathbf{I}$ is the 2×2 identity matrix, $\hat{g}(k)$ is the unit vector pointing along $\boldsymbol{g}(\boldsymbol{k})$, and $\Delta_s(\boldsymbol{k})$ and $\Delta_t(\boldsymbol{k})$ are the singlet and triplet amplitudes of the gap function, respectively. A PCAR experiment will, thus, see two gap functions, $\Delta_\pm(\boldsymbol{k}) = \Delta_s(\boldsymbol{k}) \pm \Delta_t(\boldsymbol{k})$ where each gap is defined on one of the two bands formed by the degeneracy lifting of the ASOC. In general, both the singlet and the triplet components of the order parameter can be anisotropic and can even change sign over the Fermi surface. An ABS is formed as a helical edge mode[11,39–41] for each $\boldsymbol{k}$ when $|\Delta_t(\boldsymbol{k})| > |\Delta_s(\boldsymbol{k})|$. In such a situation, on one of the bands, say $\Delta_-(\boldsymbol{k})$ can change sign [Fig. 5(b)], giving rise to nodes in the superconducting gap function for the band with negative helicity. Although at present, our understanding is clearly limited by the lack of experimental or theoretical information on the topology of the Fermi surface and the $\boldsymbol{g}(\boldsymbol{k})$ appropriate for the monoclinic structure for BiPd, based on the experimental data, we propose the following scenario. Since $\Delta_1 \sim 0.4$ meV is observed for both $I \parallel b$ and $I \perp b$ and has a similar temperature dependence in both directions, this is likely to originate from one of the gap functions associated with Δ_+. On the other hand Δ_2 and Δ_3 are likely to both be associated with a strongly anisotropic gap function (Δ_-) for which the observed gap values are different for the two different directions of current injection. Whereas, in principle, Δ_1, Δ_2, and Δ_3 could also arise from a multiband scenario containing three different bands, this is an unlikely possibility for the following reasons. First, a simple multiband scenario consisting of multiple s-wave gap functions on different Fermi sheets cannot explain the existence of the pronounced ZBCP that we observe in our data. Second, we do not observe Δ_2 and Δ_3 simultaneously in any of our spectra despite the surface roughness that produces a significant scatter in their individual gap functions for both directions of injection current. It is, therefore, unlikely that Δ_2 and Δ_3 arise from two different gap functions on different Fermi sheets. In this context, we recall that ABS is observed only when tunneling occurs in the basal plane[42] of the crystal of Sr_2RuO_4 whose OP has pure spin-triplet symmetry. On the contrary, the ABS observed here in the BiPd compound occurs for both $I \parallel b$ and $I \perp b$. We believe the main reason behind this difference is that, although pure triplet symmetry breaks the crystal symmetry, the mixed singlet-triplet OP in NCSs can restore the full crystalline symmetry,[18] and hence, OP nodes in NCSs can appear along all crystalline directions.

To summarize, we report possible evidence for the mixing of spin-triplet and spin-singlet OPs in the NCS BiPd. Furthermore, the presence of the pronounced ABS observed from the ZBCP suggests that the pair potential associated with the triplet OP is large enough to produce a sign change in at least one of the gap functions. Despite the absence of theoretical or experimental information on the Fermi surface that somehow limits our interpretation of experimental results, we believe that this observation is an important step towards realizing Majorana Fermionic modes, which are predicted to exist in the vortex core of NCSs.[8] We believe that our paper will motivate further investigations on the precise nature of the order parameter symmetry in this interesting NCS superconductor.

We thank D. Agterberg for valuable feedback on this paper.

*ramky@tifr.res.in
†pratap@tifr.res.in

[1] E. Bauer, G. Hilscher, H. Michor, C. Paul, E. W. Scheidt, A. Gribanov, Y. Seropegin, H. Noel, M. Sigrist, and P. Rogl, Phys. Rev. Lett. **92**, 027003 (2004).
[2] L. P. Gorkov and E. I. Rashba, Phys. Rev. Lett. **87**, 037004 (2001).
[3] P. A. Frigeri, D. F. Agterberg, A. Koga, and M. Sigrist, Phys. Rev. Lett. **92**, 097001 (2004).
[4] Y. Tanaka, Y. Mizuno, T. Yokoyama, K. Yada, and M. Sato, Phys. Rev. Lett. **105**, 097002 (2010).
[5] K. Yada, M. Sato, Y. Tanaka, and T. Yokoyama, Phys. Rev. B **83**, 064505 (2011).
[6] S. Fujimoto, J. Phys. Soc. Jpn. **76**, 051008 (2007).
[7] C. Iniotakis, N. Hayashi, Y. Sawa, T. Yokoyama, U. May, Y. Tanaka, and M. Sigrist, Phys. Rev. B **76**, 012501 (2007); M. Eschrig, C. Iniotakis, and Y. Tanaka, *Non-Centrosymmetric Superconductors: Introduction and Overview*, edited by E. Bauer and M. Sigrist (Springer-Verlag, Berlin Heidelberg, 2012), pp. 313–357.
[8] M. Sato and S. Fujimoto, Phys. Rev. B **79**, 094504 (2009).
[9] M. Sato, Phys. Rev. B **73**, 214502 (2006).
[10] A. B. Vorontsov, I. Vekhter, and M. Eschrig, Phys. Rev. Lett. **101**, 127003 (2008).
[11] Y. Tanaka, T. Yokoyama, A. V. Balatsky, and N. Nagaosa, Phys. Rev. B **79**, 060505(R) (2009).
[12] Y. Huang, J. Yan, Y. Wang, L. Shan, Q. Luo, W. Wang, and H.-H. Wen, Supercond. Sci. Technol. **21**, 075011 (2008).
[13] T. Klimczuk, F. Ronning, V. Sidorov, R. J. Cava, and J. D. Thompson, Phys. Rev. Lett. **99**, 257004 (2007).
[14] I. Bonalde, H. Kim, R. Prozorov, C. Rojas, P. Rogl, and E. Bauer, Phys. Rev. B **84**, 134506 (2011).
[15] C. S. Lue, T. H. Su, H. F. Liu, and B.-L. Young, Phys. Rev. B **84**, 052509 (2011).
[16] R. Onuki, A. Sumiyama, Y. Oda, T. Yasuda, R. Settai, and Y. Onuki, J. Phys.: Condens. Matter **21**, 075703 (2009).
[17] T. Akazawa, H. Hidaka, T. Fujiwara, T. C. Kobayashi, E. Yamamoto, Y. Haga, R. Settai, and Y. Onuki, J. Phys.: Condens. Matter **16**, L29 (2004)
[18] H. Q. Yuan, D. F. Agterberg, N. Hayashi, P. Badica, D. Vandervelde, K. Togano, M. Sigrist, and M. B. Salamon, Phys. Rev. Lett. **97**, 017006 (2006).

[19]S. P. Mukherjee and S. S. Mandal, Phys. Rev. B **77**, 014513 (2008).
[20]M. Nishiyama, Y. Inada, and G. Q. Zheng, Phys. Rev. Lett. **98**, 047002 (2007).
[21]B. Joshi, A. Thamizhavel, and S. Ramakrishnan, Phys. Rev. B **84**, 064518 (2011).
[22]D. Daghero and R. S. Gonnelli, Supercond. Sci. Technol. **23**, 043001 (2010).
[23]P. Raychaudhuri, D. Jaiswal-Nagar, G. Sheet, S. Ramakrishnan, and H. Takeya, Phys. Rev. Lett. **93**, 156802 (2004).
[24]R. S. Gonnelli, D. Daghero, D. Delaude, M. Tortello, G. A. Ummarino, V. A. Stepanov, J. S. Kim, R. K. Kremer, A. Sanna, G. Profeta, and S. Massidda, Phys. Rev. Lett. **100**, 207004 (2008).
[25]A. Kamlapure, M. Mondal, M. Chand, A. Mishra, J. Jesudasan, V. Bagwe, L. Benfatto, V. Tripathi, and P. Raychaudhuri, Appl. Phys. Lett. **96**, 072509 (2010).
[26]E. Yelland (private communication).
[27]Y. V. Sharvin, Zh. Eksp. Teor. Fiz. **48**, 084 (1965) [Sov. Phys. JETP **21**, 655 (1965)]; G. Wexler, Proc. Phys. Soc. London **89**, 927 (1966).
[28]Statistically, we did not find any difference between the two orthogonal directions corresponding to $I \perp b$ with the facets approximately along [001] and [100], respectively.
[29]G. E. Blonder, M. Tinkham, and T. M. Klapwijk, Phys. Rev. B **25**, 4515 (1982).
[30]R. S. Gonnelli, D. Daghero, G. A. Ummarino, V. A. Stepanov, J. Jun, S. M. Kazakov, and J. Karpinski, Phys. Rev. Lett. **89**, 247004 (2002).
[31]Attempts to fit the data in Fig. 2(a) to a single-gap model gives a strongly temperature dependent Z, which is clearly unphysical: See Supplemental Material at http://link.aps.org/supplemental/10.1103/PhysRevB.86.094520 for details.
[32]R. C. Dynes, V. Narayanamurti, and J. P. Garno, Phys. Rev. Lett. **41**, 1509 (1978).
[33]G. Sheet, S. Mukhopadhyay, and P. Raychaudhuri, Phys. Rev. B **69**, 134507 (2004).
[34]J. A. Appelbaum, Phys. Rev. **154**, 633 (1967).
[35]L. Y. L. Shen and J. M. Rowell, Phys. Rev. **165**, 566 (1968).
[36]A. Kastalsky, A. W. Kleinsasser, L. H. Greene, R. Bhat, F. P. Milliken, and J. P. Harbison, Phys. Rev. Lett. **67**, 3026 (1991); alternative explanation for this experimental observation was proposed by B. J. van Wees, P. de Vries, P. Magnée, and T. M. Klapwijk, *ibid.* **69**, 510 (1992).
[37]S. Kashiwaya and Y. Tanaka, Rep. Prog. Phys. **63**, 1641 (2000); T. Löfwander, V. S. Shumeiko, and G. Wendin, Supercond. Sci. Technol. **14**, R53 (2001).
[38]It is to be noted that few points corresponding to $I \parallel b$ fall on the branch corresponding to $I \perp b$ and vice versa. This is due to surface roughness, which limits our ability to control the direction of the current for every contact.
[39]A. P. Schnyder, P. M. R. Brydon, and C. Timm, Phys. Rev. B **85**, 024522 (2012).
[40]S. P. Mukherjee and S. S. Mandal, J. Phys.: Condens. Matter **21**, 375702 (2009).
[41]In a simplified situation where the singlet component is isotropic, i.e., $\Delta_s(\boldsymbol{k}) \equiv \Delta_s$, the condition of observing the ABS is simplified to $\Delta_t > \Delta_s$.
[42]S. Kashiwaya, H. Kashiwaya, H. Kambara, T. Furuta, H. Yaguchi, Y. Tanaka, and Y. Maeno, Phys. Rev. Lett. **107**, 077003 (2011).